A Flexible Printed Chipless RFID Tag for Concentration Measurements of Liquid Solutions

Zonghao Li[1], Sharmistha Bhadra[2]
Department of Electrical and Computer Engineering
McGill University
Montreal, Canada
[1]zonghao.li@mail.mcgill.ca, [2]sharmistha.bhadra@mcgill.ca

***Abstract*—A fully inkjet-printed flexible chipless RFID tag is presented in this paper. It is based on a coplanar waveguide (CPW) coupled to a multiresonator circuit to encode the information in the frequency domain. Two cross-polarized ultra-wideband (UWB) antennas connected to the CPW receive and transmit the signals. Three spiral resonators are used to encode a 3-bit signature. The RFID tag is applied for the wireless concentration measurements of liquid solutions by characterizing the insertion loss response. Water/isopropyl alcohol solutions with different concentrations are measured wirelessly by the tag. A capillary tube is placed on one of the resonators to allow the interaction between the sensor and the solutions. By observations of the measurements, different parameters are used to quantify the sensitivity. The change of the insertion loss at the resonant frequency $|\Delta S_{21}|$ and the shift of resonant frequency $|\Delta f_{res}|$ are used to analyze the water/isopropyl alcohol samples. A $|\Delta S_{21}|$ = 0.3dB/(20 vol%) and $|\Delta f_{res}|$ = 30 MHz/(20 vol%) have been achieved by the sensor in the concentration range of [20, 80] vol% and [40, 99] vol%, respectively.**

Keywords*—Chipless RFID, flexible electronics, liquid sensors, printed electronics.

I. Introduction

Microwave techniques for sensing liquid solutions have been studied numerously for applications such as food, beverage, medicine manufacturing and even oil industry due to their prompt and accurate response, fine accuracy, non-invasive and non-destructive natures [1]. In these techniques the variation of the concentration produces a change of the resonant frequency and quality factor (Q-factor), which provides an easy approach to analyze the liquid solutions [2].

Unlike traditional RFID tags, the chipless RFID tag has no discrete integrated circuit components on it. It has the advantages of low-cost, high durability, and compatibility with flexible substrates and printing technologies. A very important application of the chipless RFID tag is sensing [3]. This could be for sensing liquid solutions and gas concentrations [4], [5] as they are found to be significant in the fields of food, medicine manufacturing, environment monitoring, and biomedical engineering. In addition, the inkjet printing technology is an additive processes, which only deposits material on wanted areas, thereby saving more material and lowering the cost.

In this work, we present a fully inkjet-printed flexible chipless RFID tag based on the insertion loss response to measure water/isopropyl alcohol solutions with different concentrations. The RFID tag consists of a CPW coupled to three spiral resonators that encode the 3-bit information in the frequency spectrum. Two cross-polarized CPW ultra-wideband (UWB) antennas are connected to the CPW to receive and transmit the signals, respectively. The flexible substrate is a 127 μm thickness Dupton Kapton polyimide (PI) with excellent electrical properties ($\epsilon_r = 3.4$ and $tan\delta = 0.002$). The flexible conductive ink (σ = 1×10^6 S/m) as well as the inkjet printer are from Voltera. In this work, all simulations are done using ANSYS HFSS, and S-parameters are measured by the vector network analyzer (VNA, Keysight E5063A).

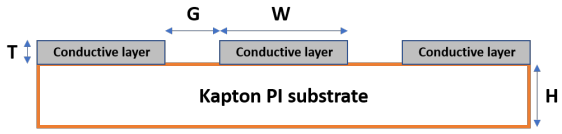

Fig. 1: CPW cross section view, where T = 50 μm, H = 127 μm, W = 5 mm, and G = 0.3 mm.

II. Design Methodologies

A. CPW and Multiresonator Circuit

Fig. 1 shows the cross-section view of the CPW transmission line used in our design based on the studies in [6], [7]. The idea of encoding the information in the insertion loss response is to use multiple resonators coupled to the CPW. Fig. 2 shows the layout of the resonator design, where three spiral resonators are located within the CPW transmission line to create a 3-bit spectrum signature. The insertion loss obtained from the HFSS simulation and the measurement results are plotted together in Fig. 3.

It can be seen that two plots in Fig. 3 are matching to each other closely, with some tolerable deviations caused by the limited accuracy of the printed. When the ink is deposited on the substrate, it tends to spread to the blank area. Therefore, the D_{res} from Fig. 2 will appear smaller on the printed tag than the designed value, leading to a resonance occurs at a slightly higher frequency. Three notches around 3.6, 4.5 and 5.3 GHz have been observed from the measurement that is generated by “res 3”, “res 2” and “res 1”, respectively. Therefore, the resonant frequency increases with the dimension shrinkage of the resonator.

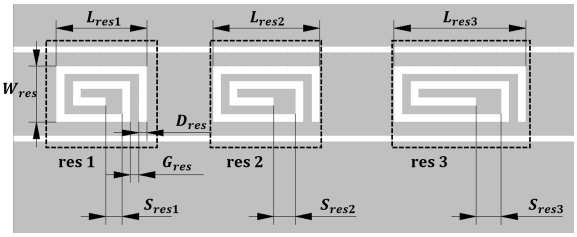

Fig. 2: Spiral resonator design, where the grey area is the conductive layer. All resonators ("res 1", "res 2" and "res 3") are centered within the CPW. L_{res1} = 5.5, L_{res2} = 6.5, L_{res3} = 8, S_{res1} = 1, S_{res2} = 1.3, S_{res3} = 1.5, W_{res} = 3.4, and D_{res} = G_{res} = 0.5, all in millimeter, and the last three parameters are the same for all resonators. From left to right, the resonators are simulated to resonate at 5.1, 4.4 and 3.5 GHz, respectively.

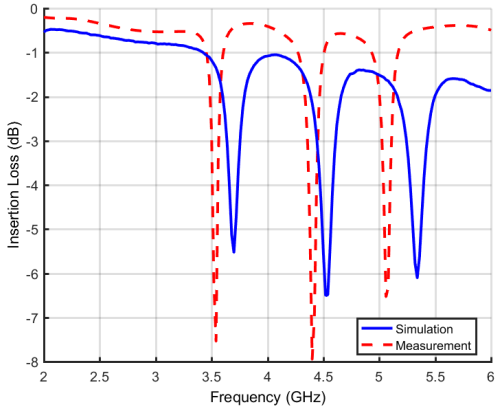

Fig. 3: Insertion loss of the CPW coupled to the three resonators, obtained from the HFSS simulation and measurement.

B. Printed Flexible UWB Antennas

The encoded frequency signature in Fig. 3 occupies a large bandwidth that requires a UWB antenna to transmit the signal with a low loss. It is also desirable to have an omnidirectional antenna so that the reader antennas can more easily receive the signal from the tag. Therefore, the monopole UWB antenna is preferable. Flexible printed monopole UWB antennas have been studied in [8]. It is shown that the ellipse-shaped planar structure has a better return loss response. Fig. 4 presents the layout of the inkjet-printed flexible UWB antenna design. The simulated and measured return loss of the antenna is shown in Fig. 5. Both plots are below the -10 dB rule of thumb across the bandwidth of interest. A simulated return loss notch is found around 2 GHz that is outside the bandwidth of interests and therefore not shown. The deviation between the simulation and measurement is majorly caused by the similar reasons happen in the CPW transmission line design. Fig. 6 shows the measured far-field radiation patterns of the UWB antenna at the central frequency 4 GHz, in both YZ and XZ planes. The UWB antenna demonstrates unidirectional radiation patterns in both planes, with a reasonable polarization purity.

III. Concentration Measurements

Fig. 7 shows the experiment setup. Two cross-polarized Vivaldi antennas interrogate the RFID tag that is place 5 cm away in the ambient environment, where a capillary tube with

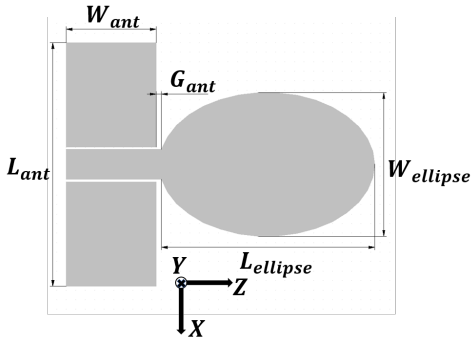

Fig. 4: Ellipse UWB antenna design with $W_{ellipse}$ = 24, $L_{ellipse}$ = 35.6, G_{ant} = 0.5, W_{ant} = 15, and L_{ant} = 40.6, all in millimeter.

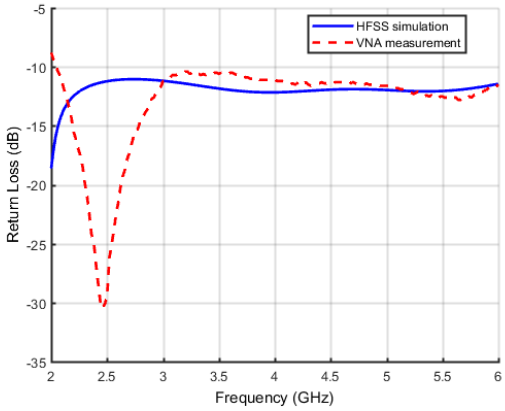

Fig. 5: Simulated and measured return loss of the UWB antenna.

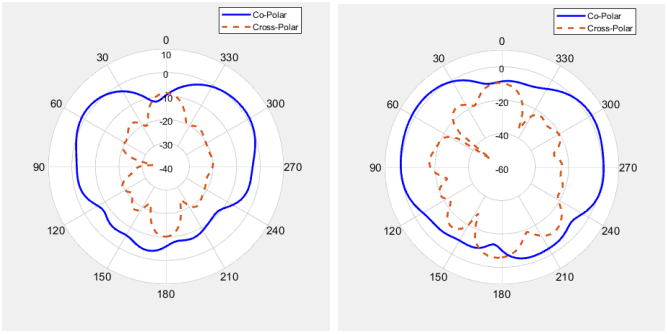

(a) (b)

Fig. 6: Measured co-polar and cross-polar far-field radiation patterns of the UWB antenna at 4 GHz in the (a) XZ and (b) YZ plane.

an inner radius r_c = 0.75 mm is centered on the top of the resonator "res 2" to achieve a better sensitivity. "res 2" is selected for the wireless measurement, because it shows a higher Q-factor than "res 1" and "res 3" in Fig. 3. The tube is filled and drained with different liquid samples by a syringe to avoid air bubbles, and the data are collected by the VNA. The experiments are operated in room temperature.

Fig. 8 shows the insertion loss response of water/isopropyl alcohol samples measured by "res 2". Noted that both Q-factor and resonant frequency change noticeably. $|\Delta S_{21}|$ and $|\Delta f_{res}|$ response versus different isopropyl alcohol concentrations are shown in Fig. 9 and 10, respectively, together with the second-order polynomial fitting result. When the isopropyl

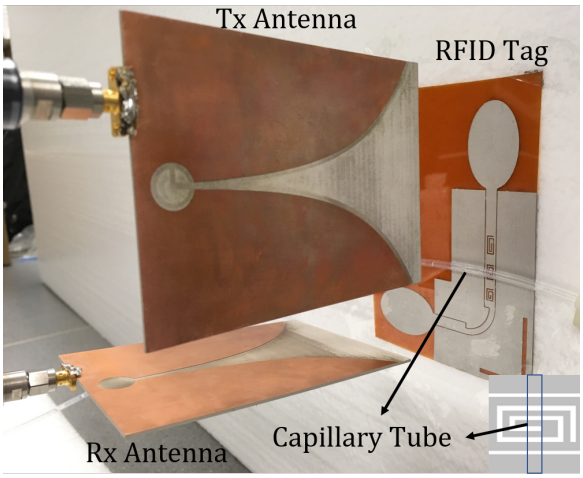

Fig. 7: Wireless measurement setup for the solutions with various concentrations. The capillary tube is place on the top the resonator "res 2".

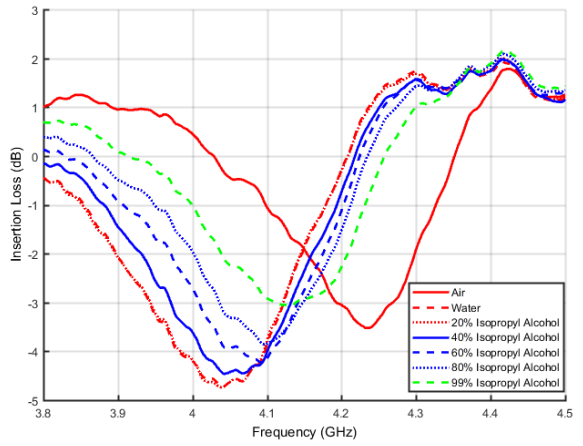

Fig. 8: Insertion loss response of the resonator "res 2" versus various water/isopropyl alcohol solutions with different concentrations in the room temperature.

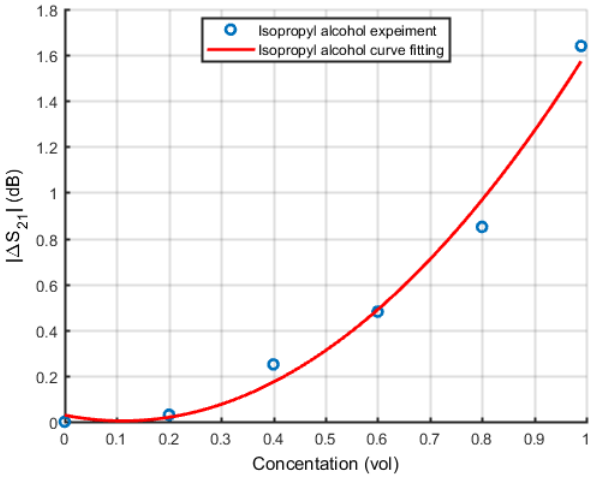

Fig. 9: Measured $|\Delta S_{21}|$ variation with isopropyl alcohol concentrations in the range [0, 99] vol% with an increment of 20 vol% per sample.

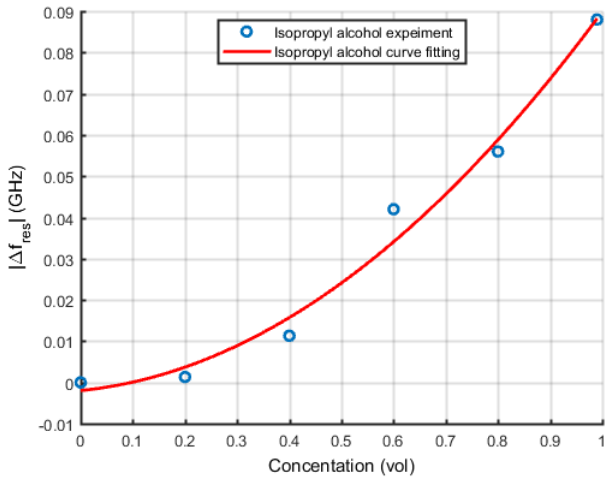

Fig. 10: Measured $|\Delta f_{res}|$ variation with isopropyl alcohol concentrations in the range [0, 99] vol% with an increment of 20 vol% per sample.

alcohol concentration is low, neither $|\Delta S_{21}|$ nor $|\Delta f_{res}|$ changes obviously. When the concentration of isopropyl alcohol is above 20 vol%, both $|\Delta S_{21}|$ and $|\Delta f_{res}|$ increase monotonically with the increase of the concentration. In Fig. 9, $|\Delta S_{21}|$ plot shows a good linearity within [20, 80] vol% concentration range with a sensitivity of 0.3 dB/(20 vol%). $|\Delta f_{res}|$ plot in Fig. 10 shows a good linearity within [40, 99] vol% concentration range with an average sensitivity of 30 MHz/(20 vol%). Across the whole testing concentration range, the second-order regression result for $|\Delta S_{21}|$ in Fig. 9 is

$$y = 2.0334x^2 - 0.453x + 0.0286 \quad (1)$$

and for ΔBW in Fig. 10 is

$$y = 0.0794x^2 + 0.0124x - 0.002 \quad (2)$$

IV. Conclusion

A flexible printed chipless RFID is applied for concentration measurements of water/isopropyl alcohol solutions. Two parameters are used to establish the correlation between the frequency response and sensitivity of the tag, the change of the insertion loss at the resonant frequency $|\Delta S_{21}|$ and the shift of resonant frequency $|\Delta f_{res}|$. Within the isopropyl alcohol concentration range of [20, 80] vol% and [40, 99] vol%, a sensitivity of 0.3 dB/(20 vol%) and 30 MHz/(20 vol%) have been realized by the tag, respectively. It should be remarked that the RFID sensor operates wirelessly in the ambient environment, and it is strongly subjected to ambient noises. Therefore, the sensitivity of the sensor is degraded, showing a limited linear range in the concentration measurements. The sensor has the potential for low-cost liquid sensing applications.

REFERENCES

[1] O. Lund Bo and E. Nyfors, "Application of microwave spectroscopy for the detection of water fraction and water salinity in water/oil/gas," *Journal of Non-Crystalline Solids*, vol. 305, pp. 345–353, 07 2002.

[2] G. Gennarelli, S. Romeo, M. R. Scarfi, and F. Soldovieri, "A microwave resonant sensor for concentration measurements of liquid solutions," *IEEE Sensors Journal*, vol. 13, no. 5, pp. 1857–1864, May 2013.

[3] N. C. Karmakar, E. M. Amin, and J. K. Saha, *Chipless RFID Sensors*. John Wiley Sons, Inc, 2016.

[4] M. H. Zarifi, M. R., M. D., and T. Thundat, "Microwave ring resonator-based non-contact interface sensor for oil sands applications," *Sensors and Actuators B: Chemical*, vol. 224, pp. 632 – 639, 2016. [Online]. Available: http://www.sciencedirect.com/science/article/pii/S092540051530527X

[5] M. H. Zarifi, A. Sohrabi, P. M. Shaibani, M. Daneshmand, and T. Thundat, "Detection of volatile organic compounds using microwave sensors," *IEEE Sensors Journal*, vol. 15, no. 1, pp. 248–254, Jan 2015.

[6] R. N. Simons, *Conventional coplanar waveguide*. IEEE, 2001. [Online]. Available: https://ieeexplore.ieee.org/xpl/articleDetails.jsp?arnumber=5237467

[7] W. Hilberg, "From approximations to exact relations for characteristic impedances," *IEEE Transactions on Microwave Theory and Techniques*, vol. 17, no. 5, pp. 259–265, May 1969.

[8] H. R. Khaleel, H. M. Al-Rizzo, D. G. Rucker, and S. Mohan, "A compact polyimide-based uwb antenna for flexible electronics," *IEEE Antennas and Wireless Propagation Letters*, vol. 11, pp. 564–567, 2012.